A molecular simulation of model liquid crystals in a strong aligning field

ENRIQUE DE MIGUEL[§], FELIPE J. BLAS[§], and ELVIRA MARTÍN DEL RÍO[†]

[§] *Departamento de Física Aplicada, Facultad de Ciencias Experimentales, Universidad de Huelva, 21071 Huelva, Spain*

[†] *Departamento de Ingeniería Eléctrica y Térmica, E.P.S. La Rábida, Universidad de Huelva, 21819 La Rábida (Huelva), Spain*

We report a computer simulation study of systems of perfectly aligned molecules interacting through the Gay-Berne (GB) potential model for two different values of the molecular anisotropy parameter κ, namely, 3 and 4.4. The models are appropriate to gauge the effects of strong aligning fields on the thermodynamics and structural properties of thermotropic liquid crystals. According to our results, one of the main effects of the external field is to increase the range of stability of the smectic A phase, which indicates the existence of a strong coupling between orientational and translational order. For the $\kappa = 3$ GB model the smectic phase, which is not stable in the absence of the field, is promoted when the molecules are constrained to be parallel. According to the simulation results, the smectic A–nematic transition is, in general, continuous; however, this transition appears to be first order at low pressure for the $\kappa = 4.4$ GB fluid model.

Keywords: liquid crystals; external field; Gay-Berne model; computer simulation

I. INTRODUCTION

Liquid crystals are known to be very sensitive to external fields [1]. Even the application of weak fields can modify the degree of orientational order, which leads to measurable changes in physical properties. The predicted effects of external fields on the thermodynamical and structural properties of liquid crystals include changes in the values of the order parameters, shifts in phase boundaries, and stabilisation of phases of different symmetry, among many others [2, 3].

For the case of fluids consisting of non-polar, non-spherical, uniaxial molecules the energy between a uniform aligning field and each single molecule may be properly modelled by

$$U_i = -\lambda\chi(\mathbf{e}\cdot\mathbf{u}_i)^2 \tag{1}$$

where λ is proportional to the intensity of the field, $\mathbf{e}$ is the direction of the field, $\mathbf{u}_i$ is a unit vector along the long

axis of molecule i, and χ is the anisotropy of the field susceptibility. Equation (1) may represent the interaction energy between an electric or magnetic field and each single molecule due to the dielectric or diamagnetic molecular anisotropy. In general, for $\chi > 0$ and fields applied along the director (average direction of molecular alignment, $\mathbf{n}$), the external field preserves the uniaxial symmetry of the phase, enhancing orientational order and thereby promoting the stabilisation of mesophases. For $\chi < 0$ the opposite trend is expected. This behaviour has been investigated within different theoretical approximations [4, 5].

For mesophases with partial translational order, such as the smectic A (SmA) phase, the effect of an orienting field is rather subttle. For fields parallel to the director of the mesophase (direction perpendicular to the SmA layers) and $\chi > 0$, the field only has a direct effect on the molecular orientations (but not on the translational degrees of freedom) and so should enhance orientational order. However, the field is expected to have an indirect effect on the smectic ordering due to the coupling between orientational and translational order parameters [6]. Whether smectic ordering is stabilised or destabilised must depend on the strength of this coupling. The effect of external fields in the SmA–nematic (N) transition has been addressed by a number of authors on the basis of different theoretical approaches, such as extensions of McMillan's molecular field theory [6, 7], Landau-de Gennes approach [6], or density functional theory [8].

The role of an orienting field on stabilising smectic phases has been considered by Luckhurst and Saielli [7] in a simulation study of the Gay-Berne (GB) model [9]. Simulations were undertaken for a fixed value of the temperature (and pressure) at which nematic behaviour was expected in the absence of the field. Increasing the strength of the external field was shown to be accompanied by an increase of the orientational order of the system. Eventually, the SmA phase was stabilised when the orientational order was sufficiently high. A further transition to a smectic B (SmB) phase was reported to take place at even stronger fields.

The effect of strong orienting fields can be analysed by considering a system of perfectly aligned molecules. Such a system would model the limiting case of freely rotating molecules in the presence of a sufficiently strong aligning field [formally, $\lambda \to \infty$ in Eq. (1)]. As the molecular long axes are constrained to point along a fixed direction in space, no isotropic (I) phase is expected, and the low-density fluid phase must be nematic. At high enough density, the system is expected to form a crystalline phase. Whether or not the system exhibits phases with partial translational order (such as smectics or columnar) at intermediate densities is not trivial.

The most extensively studied system of perfectly aligned molecules corresponds to hard spherocylinders of different shape anisotropy L/D, with L being the length of the cylindrical part of the molecule and D its diameter. The

simulation study of Stroobants *et al.* [10] has shown that a stable SmA phase is developed well before the crystallization of the system whenever the shape anisotropy L/D exceeds the value 0.5. This is to be compared with the case of systems of freely rotating spherocylinders [11–14] (no orienting external field) for which the SmA phase becomes stable only for values of L/D above 3.1 [14]. In addition, the nematic phase is stabilised for $L/D > 3.7$ [14]. The aforementioned values of the shape anisotropy fix the location of the I–SmA–solid (Cr) and I–N–SmA triple points, respectively. Interestingly, the SmA–N transition is continuous for the parallel case according to simulation [10]. On the other hand, for freely oriented spherocylinders this transition is certainly first order for $L/D \leq 5$ [13, 14], whereas it appears to be continuous for large L/D, which suggests the existence of a tricritical point at some intermediate value of L/D.

In this paper we investigate the effect of strong fields on the phase behaviour of model thermotropic liquid crystals. Certainly, models based on hard particles are of considerable importance for the study of systems, such as anisotropic colloids or rodlike virus, where excluded volume interactions are the driving mechanism for phase transitions, but are not suitable for the study of temperature-driven phase transitions. We choose systems consisting of elongated parallel molecules interacting through the standard GB [9] potential model. This model has been widely used in simulation [15–21] and theoretical [22–24] studies of the phase behaviour in the abscence of external fields (see Ref. [25] for a recent review on the subject of computer simulation of GB systems). The perfectly oriented GB model has been previously considered in a simulation study of the viscosity in the vicinity of the SmA–N transition [26]. This model has also been considered to test a perturbation theory for nematics [27]. More recently, Józefowicz *et al.* [28] have studied the SmA–N phase boundary of the perfectly aligned $\kappa = 3$ GB model using local density functional theory and Monte Carlo simulation.

The rest of the paper is organised as follows. We present the molecular model in section II, where we also highlight the most relevant features of the phase diagram of the model fluids in the absence of external fields. Details of the simulation methodology are given in section III. The results and discussion are presented in section IV; and the conclusions are made in section V.

II. THE MODEL

In the GB interaction model [9], molecules are considered as rigid units with axial symmetry. Molecule ith is represented by the position vector $\mathbf{r}_i$ of its centre of mass and a unit vector $\hat{\mathbf{u}}_i$ along its symmetry axis. The intermolecular potential energy between two arbitrary molecules i and j is given by

$$U_{ij}(\mathbf{r}_{ij},\hat{\mathbf{u}}_i,\hat{\mathbf{u}}_j) = 4\epsilon(\hat{\mathbf{r}}_{ij},\hat{\mathbf{u}}_i,\hat{\mathbf{u}}_j)\left[\left(\frac{\sigma_0}{r_{ij}-\sigma(\mathbf{r}_{ij},\hat{\mathbf{u}}_i,\hat{\mathbf{u}}_j)+\sigma_0}\right)^{12} - \left(\frac{\sigma_0}{r_{ij}-\sigma(\mathbf{r}_{ij},\hat{\mathbf{u}}_i,\hat{\mathbf{u}}_j)+\sigma_0}\right)^{6}\right] \tag{2}$$

where r_{ij} is the distance between the centres of mass of molecules i and j, and $\hat{\mathbf{r}}_{ij} = \mathbf{r}_{ij}/r_{ij}$ is a unit vector along the intermolecular vector $\mathbf{r}_{ij} = \mathbf{r}_i - \mathbf{r}_j$. ϵ is a measure of the strength of the interactions, and σ is the distance at which the intermolecular potential vanishes. Both ϵ and σ depend on $\hat{\mathbf{u}}_i$, $\hat{\mathbf{u}}_j$, and $\hat{\mathbf{r}}_{ij}$. σ_0 in Eq. (2) defines the smallest molecular diameter.

In the perfectly aligned GB model, all molecules are oriented in the same direction defined here by a unit vector $\hat{\mathbf{u}}$. In this case, σ and ϵ depend only on $\cos\theta = \hat{\mathbf{r}}_{ij}\cdot\hat{\mathbf{u}}$ and are explicitly given by

$$\sigma(\cos\theta) = \sigma_0\left[1-\left(\frac{2\chi}{1+\chi}\right)\cos^2\theta\right]^{-1/2} \tag{3}$$

and

$$\epsilon(\cos\theta) = \epsilon_0[(1-\chi^2)^{-1/2}]^{\nu}\left[1-\left(\frac{2\chi'}{1+\chi'}\right)\cos^2\theta\right]^{\mu}, \tag{4}$$

where $\chi = (\kappa^2-1)/(\kappa^2+1)$ and $\chi' = (\kappa'^{1/\mu}-1)/(\kappa'^{1/\mu}+1)$. Here, κ and κ' are two anisotropy parameters with κ being a measure of the length-to-breadth ratio of the molecule and κ' being the ratio of the potential well depths for the side-by-side and end-to-end configurations. The anisotropy of the well depth ϵ is also controlled by two additional parameters μ and ν. Finally, ϵ_0 in Eq. (4) sets the energy scale of the interactions.

The GB interactions define a family of potential models each characterised by the choice of parameters κ, κ', μ, and ν. In their seminal work [9], Gay and Berne considered the anisotropy parameters $\kappa = 3$, $\kappa' = 5$, along with the values $\mu = 2$ and $\nu = 1$ (hereafter referred to as the $\kappa = 3$ GB model). For this choice of parameters the nematic phase becomes stable above a I–N–Cr triple point. According to simulation [20], this triple point is characterised by a pressure value of $P_t = 2.70$ (expressed in conventional reduced units of ϵ_0/σ_0^3) and a temperature value of $T = 0.85$ (expressed in reduced units of ϵ_0/k_B, with k_B being Boltzmann's constant). At an even lower temperature ($T \approx 0.47$) there exists a critical point below which vapour-(isotropic) fluid separation takes place over a rather small range of temperatures [20]. No other liquid crystalline phases are found for this set of parameters.

As a matter of fact, the value $\kappa = 3$ for the molecular elongation parameter seems to be close to the (lower) limit of

stability of the SmA phase; as shown by Brown *et al.* [18], slightly larger values of κ tend to promote smectic ordering. This is consistent with simulations of the GB model with $\kappa = 4.4$, $\kappa' = 20$ and exponent parameters $\mu = \nu = 1$ [19, 21], hereafter referred to as the $\kappa = 4.4$ GB model.

According to simulation [21], the freely rotating $\kappa = 4.4$ GB model exhibits a Cr phase at low temperatures, I phase at high temperatures, and different mesophases at intermediate temperatures depending on the applied pressure. The smectic phase enters the phase diagram above a certain pressure ($P \approx 0.4$). At pressures above this value, the system follows the phase sequence Cr $\rightarrow$ SmA $\rightarrow$ I with increasing temperature. At still higher pressures ($P \gtrsim 1.25$), nematic ordering is developed between the SmA and I phases. At sufficiently high pressure, the smectic phase turns unstable and the Cr phase melts directly into a N liquid.

III. SIMULATION DETAILS

We have used constant-pressure Monte Carlo (MC) simulation to investigate the behaviour of two different parametrizations of the GB model under strong (effectively infinite) aligning fields. All particles were oriented in the same direction, here taken to be the z-axis. In order to be consistent with previous simulations for freely oriented GB systems, the intermolecular interactions for the $\kappa = 3$ GB model were truncated and shifted at $r_c = 4.0\sigma_0$, whereas the interactions for the $\kappa = 4.4$ GB model were truncated (but not shifted) at $r_c = 5.5\sigma_0$. Standard periodic boundary conditions were used.

Sequences of constant-pressure MC simulations were initiated at low temperatures from a crystalline structure consisting of six layers with hexagonal in-plane order arranged perpendicular to z following an ABC sequence. Each layer consisted of 15×18 molecules ($N = 1620$ molecules). The system was heated by slowly increasing the input temperature in small steps. In order to check for hysteresis at the various transitions, some of the isobars were started from a fluid (nematic) configuration at high temperature and the system was slowly cooled by decreasing the input temperature in small steps until crystallization. The simulations were organised in cycles, each cycle consisting of N attempts to displace the molecules and two or three trial volume fluctuations, as explained elsewhere [21]. At each input temperature, the system was typically equilibrated for 75 000 cycles and thermodynamic averages were collected over 25 000 additional cycles, although near a transition runs several times longer were performed.

The nature of the different phases was probed by computing a number of order parameters. The onset of a density

modulation along the z-axis was monitored by calculating the translational order parameter $\tau = \max\{\tau(q)\}$, with

$$\tau(q) = |\langle \exp(iqz) \rangle| \tag{5}$$

where q is the magnitude of the wave vector defined as $q = 2\pi/d$, and d is the (as yet unknown) layer spacing. The evaluation of τ and d was performed as in our previous work [21]. According to its definition, τ vanishes for the N phase and takes values between 0 and 1 for phases with translational order along the z-axis (smectic and crystalline phases).

Translational in-plane order was probed by computing the bond orientational order parameter ψ_6 [19, 21, 29]. This parameter was calculated by averaging the local bond orientational order $\psi_6(\mathbf{r}_i)$ over the whole system [19, 21]. ψ_6 vanishes for liquid-like in-plane order, such as that exhibited by I, N and SmA phases and takes values between 0 and 1 for phases with hexagonal in-plane order, such as the Cr and SmB phases.

All quantites given below are expressed in conventional reduced units, with σ_0 and ϵ_0 being the units of length and energy, respectively. Thus, the temperature is given in units of ϵ_0/k_B, the pressure is in units of ϵ_0/σ_0^3, and the number density is in units of σ_0^{-3}.

IV. RESULTS

A. $\kappa = 4.4$ GB model

We show in figure 1 the average number density as a function of temperature as obtained from simulations of the perfectly aligned $\kappa = 4.4$ GB system along different constant-pressure paths, namely $P = 2.0, 1.0, 0.4$, and 0.2. For each value of the pressure, a solid configuration was equilibrated at low temperature and subsequently heated in small temperature jumps. The solid phase was seen to melt via a first-order transition at temperatures $T = 2.25 \pm 0.01$ ($P = 2.0$), $T = 1.71 \pm 0.01$ ($P = 1.0$), $T = 1.31 \pm 0.01$ ($P = 0.4$), and $T = 1.16 \pm 0.01$ ($P = 0.2$). According to the behaviour of the order parameters with varying temperature (see figures 2 and 3), the high-temperature phase was seen to be characterised in all cases by $\psi_6 \approx 0$ and $\tau \neq 0$. It was concluded that the solid phase melted into a SmA phase at all the pressures investigated here. The SmA phase was seen to undergo a further transition at higher temperatures, signalled by a discontinuity in the slope of the equation of state (see figures 1(a)–(d)) at temperatures $T = 2.62 \pm 0.03$ ($P = 2.0$), $T = 2.13 \pm 0.02$ ($P = 1.0$), $T = 1.66 \pm 0.01$ ($P = 0.4$), and $T = 1.40 \pm 0.02$ ($P = 0.2$). As shown in figure 2, the translational order parameter τ is seen to decrease steadily with increasing temperature and

to vanish at the quoted transition temperatures. These temperatures therefore locate the SmA–N transitions at each of the pressures investigated. No density jump was seen to accompany the SmA–N transition within the accuracy of the simulations. This, along with the fact that τ vanishes in an essentially continuous way, points to the conclusion that the SmA–N transition is continuous. Independent series of simulations were started by generating a nematic configuration at high temperature. Once equilibrated, this configuration was slowly cooled in small temperature jumps at constant pressure. Eventually, the N phase was seen to give way to smectic layering at essentially the same temperatures (within statistical uncertainties) at which the SmA–N transitions were observed along the heating series. On the contrary, freezing of the SmA phase into a crystalline structure was found to take place at significantly lower temperatures. This is as expected for a strongly first-order transition. A similar behaviour has been reported for the Cr–SmA transition in systems of freely rotating GB molecules [21]. The low-temperature solid phase obtained on cooling seems to quench defects in the crystalline structure and this results in a larger available volume per molecule, or lower overall number density, when compared to a defect-free crystalline configuration at the same temperature, as can be observed in figure 1.

It is worth mentioning that we observed no transition from the crystal phase to any intermediate SmB phase in the range of pressures considered here. A possible stabilisation of the SmB phase was ruled out after analysing a number of transversal distribution functions, such as the in-layer positional distributions $g_{nn}(R)$ and the interlayer distribution funcions $g_{nm}(R)$, where n and m are integers labelling the layers, and R is the projection onto the layer plane of the intermolecular vector between a molecular pair belonging to the same ($n = m$) or to different ($n \neq m$) layers.

The corresponding equations of state for the $\kappa = 4.4$ GB model of freely rotating molecules have been included in figure 1 for comparison. Appart from the trivial absence of a high-temperature I phase in systems of parallel molecules, the main effects of the strong external field are to make the Cr and SmA phases stable at higher temperatures and to increase the temperature range of stability of the SmA phase. Smectic ordering is also promoted in the low-pressure region where no SmA is observed in the absence of the orienting field.

We now turn to examine the variation with temperature of the layer spacing. Following Aoki and Yonezawa [30], we have computed the average interlayer distance d_z, and the average in-layer pair distance d_{xy}. These are defined as $d_z = \langle L_z/N_z \rangle$, with L_z being the length of the simulation box in the z direction, and N_z the number of layers; and $d_{xy} = \langle (S_{xy}/N_{xy})^{1/2} \rangle$, with S_{xy} being the area of the cross section of the simulation box, and N_{xy} the average number of particles per layer ($N_{xy} = N/N_z$, with N being the total number of particles). The values of d_z calculated

in this way were found to agree, within numerical uncertainties, with the values of d obtained from the wave vector q that maximises $\tau(q)$ in equation (5).

The variation of the layer spacing d_z with temperature along the isobars considered in this work is shown in figure 4(a). d_z is seen to increase as the solid phase is heated up. This is the expected behaviour due to an expansion of the crystalline structure at constant pressure. At a given temperature, the value of d_z becames larger with decreasing values of the pressure. Also, $d_z < \kappa$ in the solid phase at all pressures and temperatures, this being an indication of interdigitation between adjacent layers. A similar behaviour is found for d_z along the SmA phase, although the temperature dependence of d_z seems weaker. According to figure 4(a), $d_z > \kappa$ at low pressures and $d_z \lesssim \kappa$ at higher pressures, this indicating again interdigitation between adjacent layers in the SmA phase. The layer spacing is seen to increase at the Cr–SmA transition. This is to be compared with the behaviour found for systems of freely rotating GB molecules, for which d_z has been reported to decrease at the Cr–SmA transition [21]. In such a case, the transition must be accompanied by an expansion of the layers to account for the increase of the volume at melting. For the perfectly aligned GB model, the observed expansion of the system along z could in principle be followed by either a compression or expansion of the layers at the Cr–SmA transition. An inspection of figure 4(b) shows that the melting of the crystal layers into smectic layers is accompanied by an expansion of the layers at all pressures.

The phase behaviour of the perfectly aligned $\kappa = 4.4$ GB model is summarised in figure 5, where we show an approximate phase diagram of the model in the pressure-temperature plane. The Cr–SmA line in the figure represents the loci where the Cr phase turns mechanically unstable against the SmA phase on heating. Considering the hysteresis around this transition, this line does not correspond to the melting line: a proper calculation of the latter would have required computation of the free energies, which is outside the scope of this work. According to this, the region of thermodynamical stability of the SmA phase is expected to widen towards lower temperatures. Considering the phase behaviour in the absence of the external field [21], one can anticipate that for parallel GB molecules, the SmA phase must also turn unstable at sufficiently high pressures. This point, however, was not investigated further. On the other hand, some exploratory runs were performed in the low-pressure ($P < 0.4$) region. The corresponding variation of the average number density with temperature is shown in figure 6 for some values of the pressure. The most singular feature is that the SmA–N transition seems to become first order in this region: the transition appears to be accompanied by a density jump, which becomes larger with decreasing values of the pressure. A similar discontinuity at the transition was exhibited by the translational order parameter. These results suggest the existence of a pressure-induced tricritical point where the transition changes from first order (at lower pressure) to continuous (at higher

pressure). Tricritical behaviour at the SmA–N transition induced by pressure has been observed experimentally [31]. From the simulation data, the tricritical point can be approximately located at $T_{\rm tc} \approx 1.20$ $P_{\rm tc} \approx 0.11$ (see figure 5).

Eventually, the Cr phase melts directly into the N phase at very low pressures, the transition not being mediated by smectic ordering. As found for GB systems in the absence of external field [21], the SmA phase becomes unstable at very low pressure even in the presence of a strong orienting field.

B. The $\kappa = 3$ GB model

We next considered systems of parallel molecules interacting through the $\kappa = 3$ GB model. A similar procedure was used for the constant-pressure Monte Carlo simulations carried out at $P = 1.0$ and 0.3. In both cases, a defect-free crystalline structure was equilibrated at low temperature and heated up in small jumps in temperature. Figures 7 and 8 show the variation with temperature of the average density and translational order parameter τ along both isobars. As shown in these figures, the crystal phase melts at temperatures $T = 1.24 \pm 0.01$ ($P = 1.0$), and $T = 0.98 \pm 0.01$ ($P = 0.4$). The phase on the high-temperature side of the transition at $P = 1.0$ seemed to be a SmA liquid characterised by a relatively small value of τ (≈ 0.40). On increasing the temperature, the translational order along z was lost at $T = 1.32$. Considering the large fluctuations of τ for temperatures between 1.24 and 1.32, it was difficult to assess whether the system displayed smectic ordering in this range. Beyond $T = 1.32$, the fluid was clearly nematic. A similar scenario was found at the lower pressure: at $P = 0.4$, the nematic phase was observed for temperatures beyond $T = 1.00$. Whether a SmA phase was stable over a very narrow temperature range or not stable at all was hard to decide in the light of these results. On the other hand, after slowly cooling down a nematic configuration (previously equilibrated at high temperature) a transition to the SmA was observed at temperatures $T = 1.32 \pm 0.02$ ($P = 1.0$) and $T = 1.00 \pm 0.02$ ($P = 0.4$). The SmA phase was found to freeze into a crystal structure at lower temperatures, as can be observed in figures 7 and 8. As found for the $\kappa = 4.4$ GB system, the SmA–N transition is likely to be continuous, whereas the Cr–SmA transition is strongly first order and is accompanied by hysteresis. Also as before, the melting temperature (not calculated here) must be bracketed by the temperatures at which the Cr (SmA) turns mechanically unstable against the SmA (Cr) phase on heating (cooling). We therefore conclude that a thermodynamically stable SmA phase develops in between the Cr and N phase at both pressures. We recall that in the absence of the external orienting field, the $\kappa = 3$ GB fluid does not exhibit smectic ordering.

As for the variation of d_z and d_{xy} at the Cr–SmA transition, the system was found to exhibit the same behaviour as that already mentioned for the $\kappa = 4.4$ GB system.

V. CONCLUSIONS

We have investigated the effects of a strong aligning field on the phase behaviour of prototype models of thermotropic liquid crystals. This has been accomplished by carrying out constant-pressure Monte Carlo simulations of systems of perfectly aligned molecules interacting through the Gay-Berne potential. Two different sets of parameters have been considered: (i) $\kappa = 4.4$, $\kappa' = 20$, $\mu = \nu = 1$ (the $\kappa = 4.4$ GB model); and (ii) $\kappa = 3$, $\kappa' = 5$, $\mu = 2$, and $\nu = 1$ (the $\kappa = 3$ GB model). In the absence of external fields, the main difference between these models is that, according to simulation, the former stabilises the SmA phase, whereas this phase is unstable in the GB $\kappa = 3$ model.

The application of a strong aligning field is seen to promote the stabilisation of phases with translational order. This behaviour results from a strong coupling between the orientational and translational order. One of the effects of the external field is to increase the range of stability of the SmA phase. In addition, the field promotes the formation of the SmA phase in the $\kappa = 3$ GB model fluid. The SmA–N transition is found to be continuous for most values of the pressure; however, it seems to proceed discontinuously at very low pressure for the $\kappa = 4.4$ GB model. The simulation results indicate that the Cr–SmA transition is accompanied by an increase of the layer spacing due to an expansion of the system in the direction normal to the layers. The reverse behaviour has been reported for GB systems in the absence of external field.

Acknowledgement

Financial support is due to project number FIS2004-06627-C02-01 of the Spanish Dirección General de Investigación. Additional support from Universidad de Huelva and Junta de Andalucía is also acknowledged.

[1] P.G. de Gennes, J. Prost. *The Physics of Liquid Crystals*, 2nd edn, Clarendon Press, Oxford (1993).

[2] L.M. Blinov. In *Physical Properties of Liquid Crystals*, D. Demus, J. Goodby, G.W. Gray, H.-W. Spiess and V. Vill (Eds), chap. 9, Willey-VCH, Weinheim (1999).

[3] D.A. Dunmur, P. Palffy-Muhoray. *J. Phys. Chem.*, **92**, 1406 (1988).

[4] A.R. Khoklov, A.N. Semenov. *Macromolecules*, **15**, 1272 (1982).

[5] S. Varga, G. Jackson, I. Szalai. *Mol. Phys.*, **93**, 377 (1998).

[6] H. Hama. *J. Phys. Soc. Jap.*, **54**, 2204 (1985).

[7] G.R. Luckhurst, G. Saielli. *J. Chem. Phys.*, **112**, 4342 (2000).

[8] H. Graf, H. Löwen. *J. Phys.: Condens. Matter*, **11**, 1435 (1999).

[9] J.G. Gay, B.J. Berne. *J. Chem. Phys.*, **74**, 3316 (1981).

[10] A. Stroobants, H.N.W. Lekkerkerker, D. Frenkel. *Phys. Rev. Lett.*, **57**, 1452 (1986); *Phys. Rev. A*, **36**, 2929 (1987).

[11] D. Frenkel. *J. Phys. Chem.*, **92**, 3280 (1988).

[12] J.A.C. Veerman, D. Frenkel. *Phys. Rev. A*, **41**, 3237 (1990).

[13] S.C. McGrother, D.C. Williamson, G. Jackson. *J. Chem. Phys.*, **104**, 6755 (1996).

[14] P. Bolhuis, D. Frenkel. *J. Chem. Phys.*, **106**, 666 (1997).

[15] G.R. Luckhurst, R.A. Stephens, R.W. Phippen. *Liq. Cryst.*, **8**, 451 (1990).

[16] E. de Miguel, L.F. Rull, M.K. Chalam, K.E. Gubbins. *Mol. Phys.*, **74**, 405 (1991).

[17] E. de Miguel, E. Martín del Río, J.T. Brown, M.P. Allen. *J. Chem. Phys.*, **105**, 4234 (1996).

[18] J.T. Brown, M.P. Allen, E. Martín del Río, E. de Miguel. *Phys. Rev. E*, **57**, 6685 (1998).

[19] M.A. Bates, G.R. Luckhurst. *J. Chem. Phys.*, **110**, 7087 (1999).

[20] E. de Miguel, C. Vega. *J. Chem. Phys.*, **117**, 6613 (2002).

[21] E. de Miguel, E. Martín del Río, F.J. Blas. *J. Chem. Phys.*, **121**, 11183 (2004).

[22] J. Ram, R.C. Singh, Y. Singh. *Phys. Rev. E*, **49**, 5117 (1994).

[23] E. Velasco, A.M. Somoza, L. Mederos. *J. Chem. Phys.*, **102**, 8107 (1995).

[24] E. Velasco, L. Mederos. *J. Chem. Phys.*, **109**, 2361 (1998).

[25] C.M. Care, D.J. Cleaver. *Rep. Prog. Phys.*, **68**, 2665 (2005).

[26] L. Bennett, S. Hess, C. Pereira Borgmeyer, T. Weider. *Int. J. Thermophys.*, **19**, 1143 (1998).

[27] W.L. Wagner, L. Bennett. *Mol. Phys.*, **94**, 571 (1998).

[28] W. Józefowicz, G. Cholewiak, L. Longa. *Phys. Rev. E*, **71**, 032701 (2005).

[29] K.J. Strandburg. In *Bond-orientational Order in Condensed Matter Systems*, K.J. Strandburg (Ed), chap. 2, Springer, New York (1992).

[30] K.M. Aoki, F. Yonezawa. *Phys. Rev. E*, **46**, 6541 (1992).

[31] T. J. McKee, J. R. McColl. *Phys. Rev. Lett.*, **34**, 1076 (1975).

List of figures

Figure 1.

Variation of the number density $\rho\sigma_0^3$ with reduced temperature T (in units of ϵ_0/k_B) as obtained from simulations of the $\kappa = 4.4$ GB model at constant pressure P (in units of ϵ_0/σ_0^3). (a) $P = 2.0$, (b) $P = 1.0$, (c) $P = 0.4$, and (d) $P = 0.2$. Circles are data for systems of parallel molecules, and squares are for systems with no external orienting field.

Figure 2.

Variation of the translational order parameter τ with reduced temperature T as obtained from simulations of the parallel $\kappa = 4.4$ GB model along heating series at constant pressure.

Figure 3.

Variation of the bond orientational order parameter ψ_6 with reduced temperature T as obtained from simulations of the parallel $\kappa = 4.4$ GB model along heating series at constant pressure.

Figure 4.

(a) Variation of the interlayer spacing d_z (in units of $\kappa\sigma_0$) with reduced temperature T along the crystal and smectic A phases as obtained from simulations of the parallel $\kappa = 4.4$ GB model along heating series at constant pressure. (b) The same as in (a), but for the in-layer spacing d_{xy} (in units of σ_0).

Figure 5.

Approximate phase diagram for the parallel $\kappa = 4.4$ GB model in the P–T plane showing nematic (N), smectic A (SmA), and crystal (Cr) phases. Open symbols correspond to the (approximate) transition temperatures obtained on heating. Continuous lines are a guide to the eye. Discontinuous are plausible extrapolations. Filled symbol is for the approximate location of the tricritical point on the SmA–N transition line.

Figure 6. Variation of the number density $\rho\sigma_0^3$ with reduced temperature T (in units of ϵ_0/k_B) as obtained from simulations of the parallel $\kappa = 4.4$ GB model at low pressures. Open symbols correspond to data obtained along

heating series; filled symbols are data obtained on cooling from a high-temperature nematic liquid.

Figure 7.

Variation of the number density $\rho\sigma_0^3$ with reduced temperature T (in units of ϵ_0/k_B) as obtained from simulations of the parallel $\kappa = 3$ GB model at constant pressure P (in units of ϵ_0/σ_0^3). Filled symbols correspond to data obtained along the heating series; open symbols are data along the cooling series.

Figure 8.

Variation of the translational order parameter τ with reduced temperature T (in units of ϵ_0/k_B) as obtained from simulations of the parallel $\kappa = 3$ GB model at constant pressure P (in units of ϵ_0/σ_0^3). Open symbols correspond to data obtained along the heating series; filled symbols are data along the cooling series.

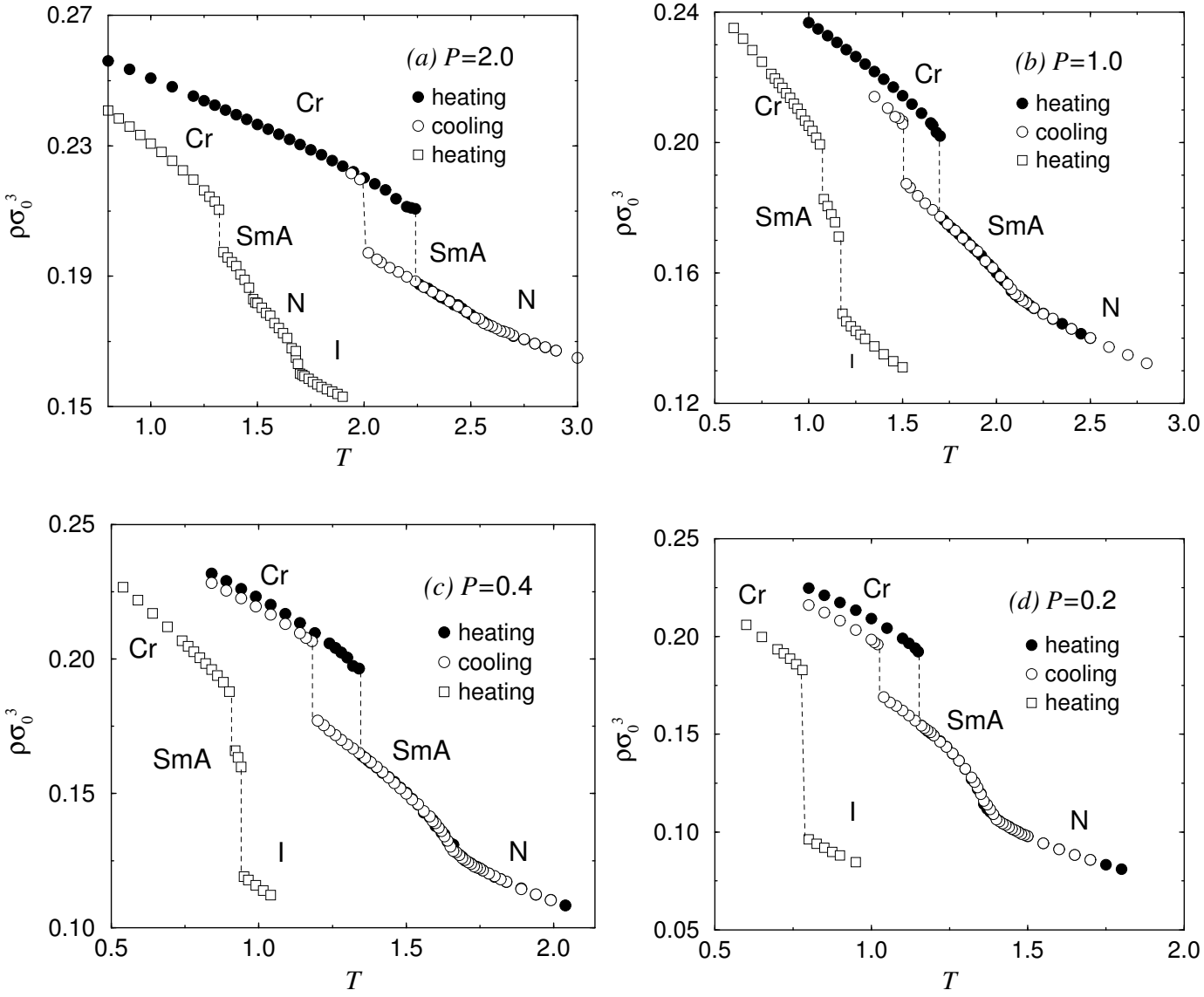
(a) P=2.0
heating
cooling
heating
Cr
Cr
SmA
SmA
N
N
I
(b) P=1.0
heating
cooling
heating
Cr
Cr
SmA
SmA
N
I
(c) P=0.4
heating
cooling
heating
Cr
Cr
SmA
SmA
N
I
(d) P=0.2
heating
cooling
heating
Cr
Cr
SmA
I
N
ρσ0^3
T

Figure 1

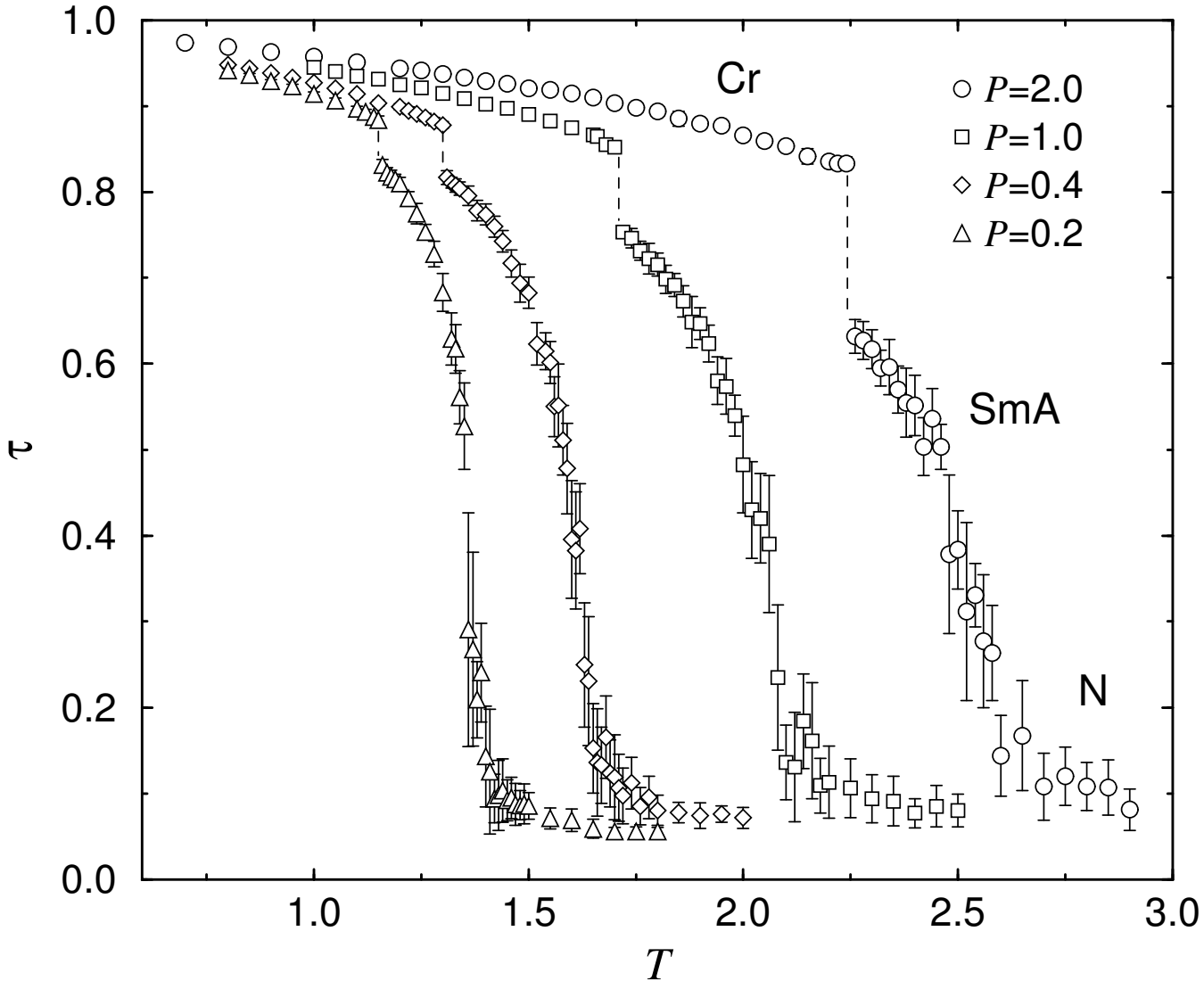

Figure 2

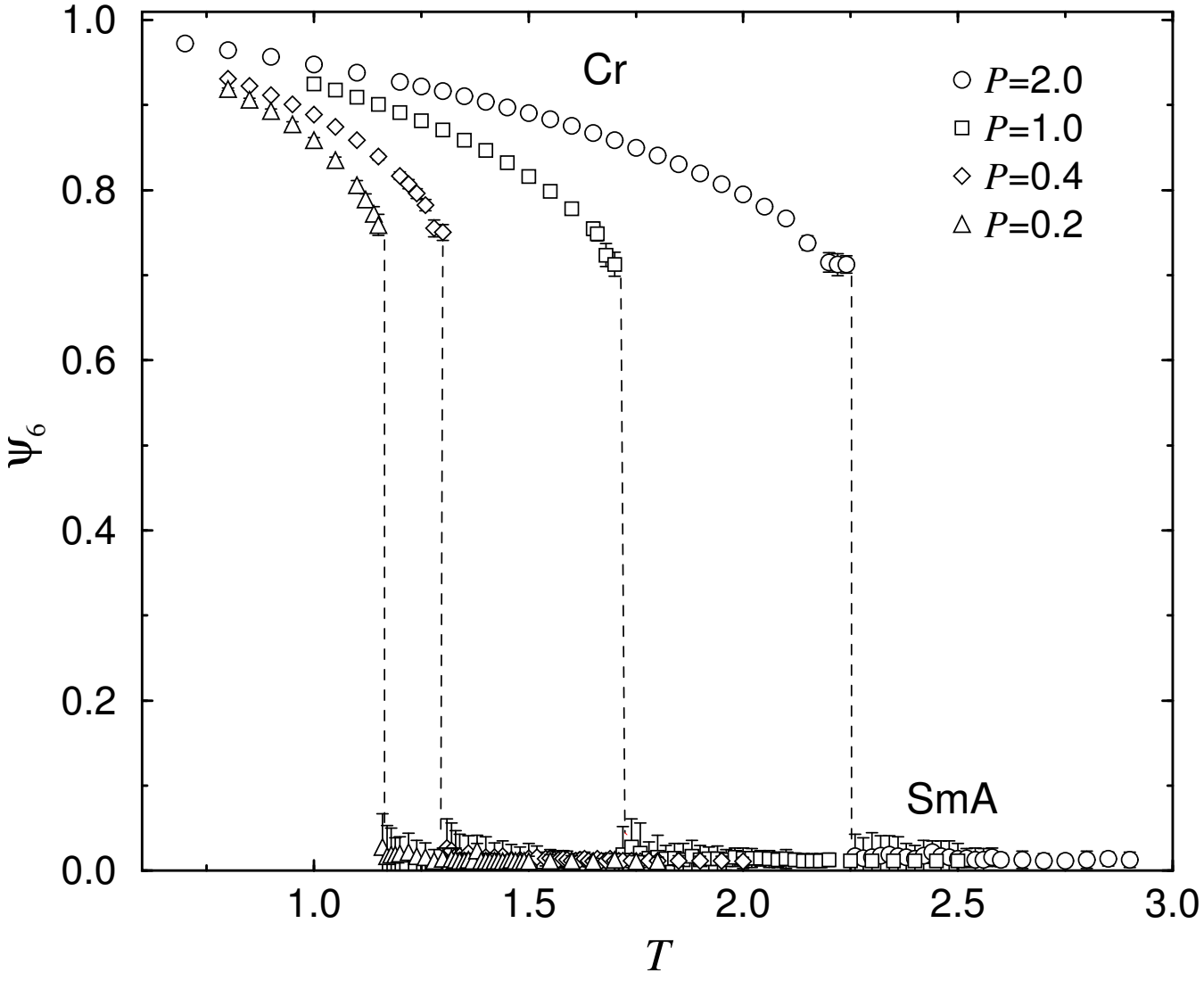

Figure 3

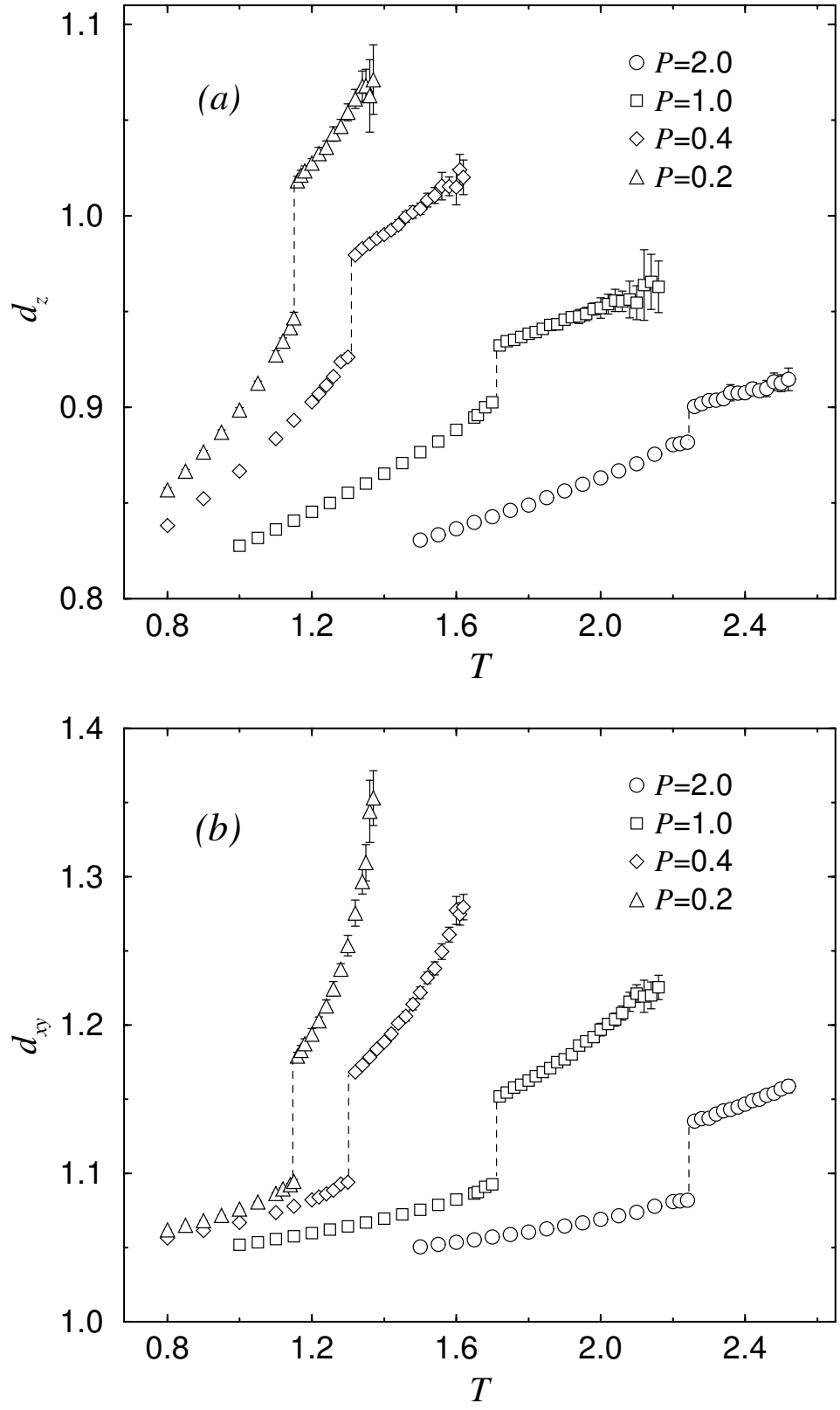

Figure 4

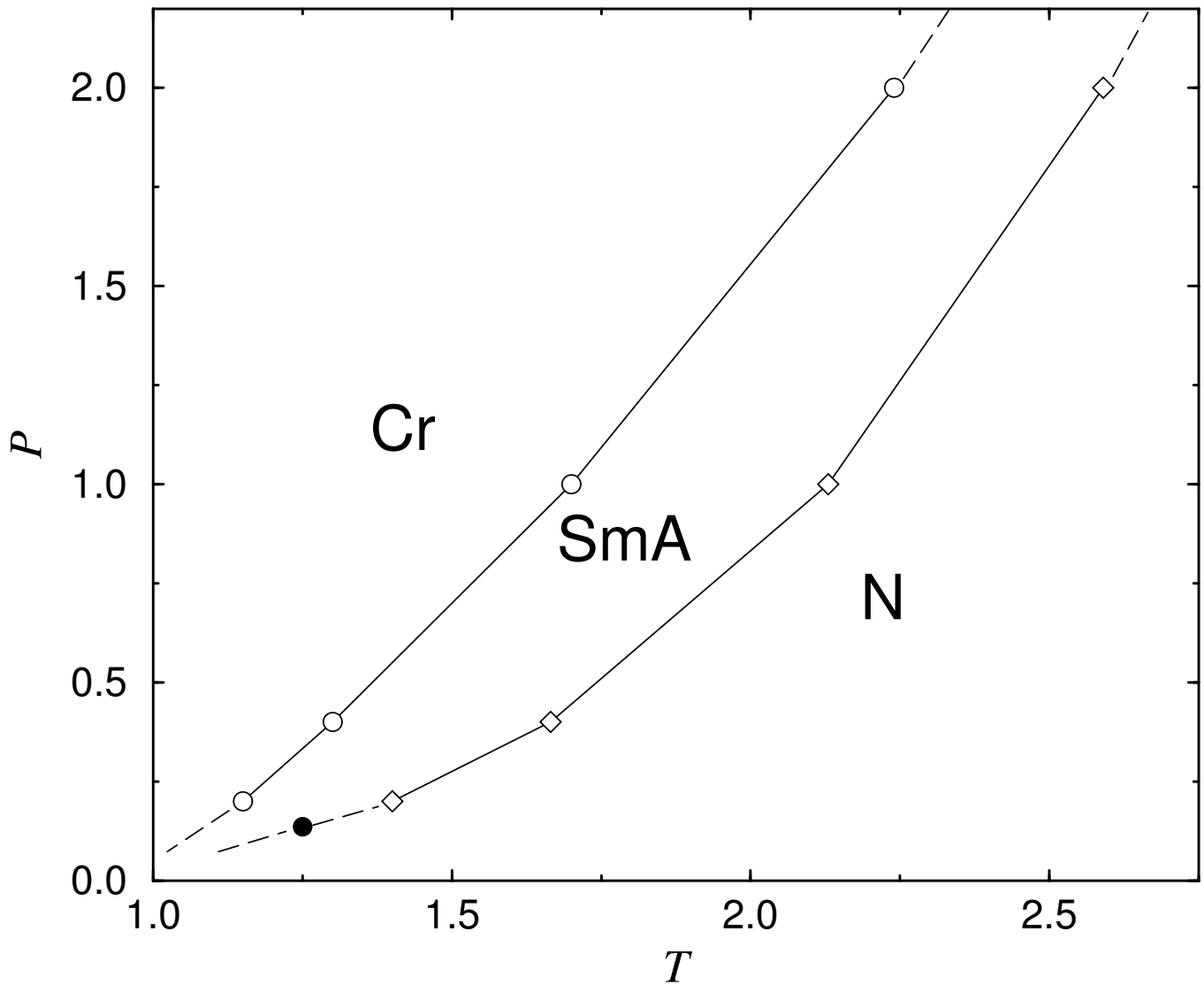

Figure 5

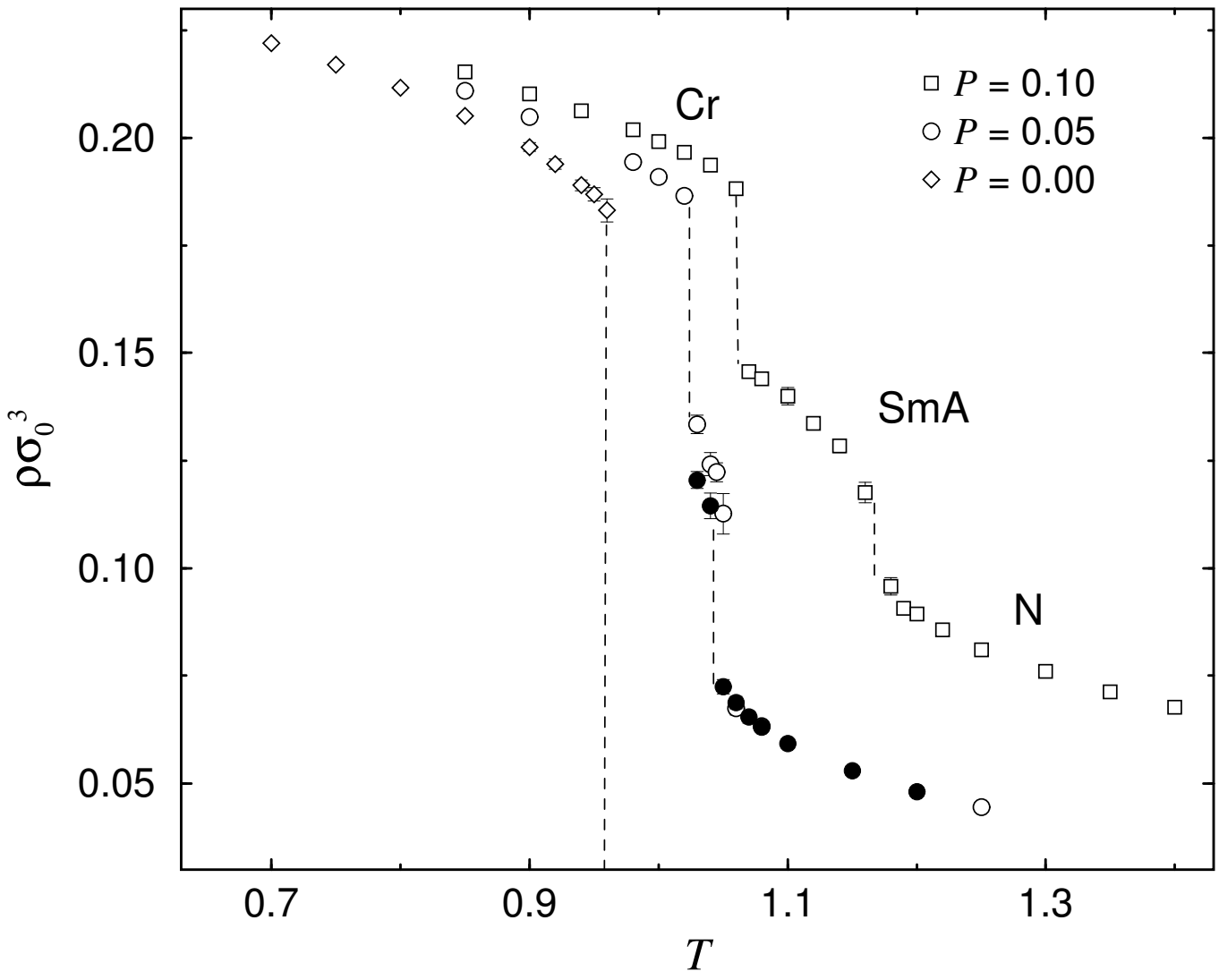

Figure 6

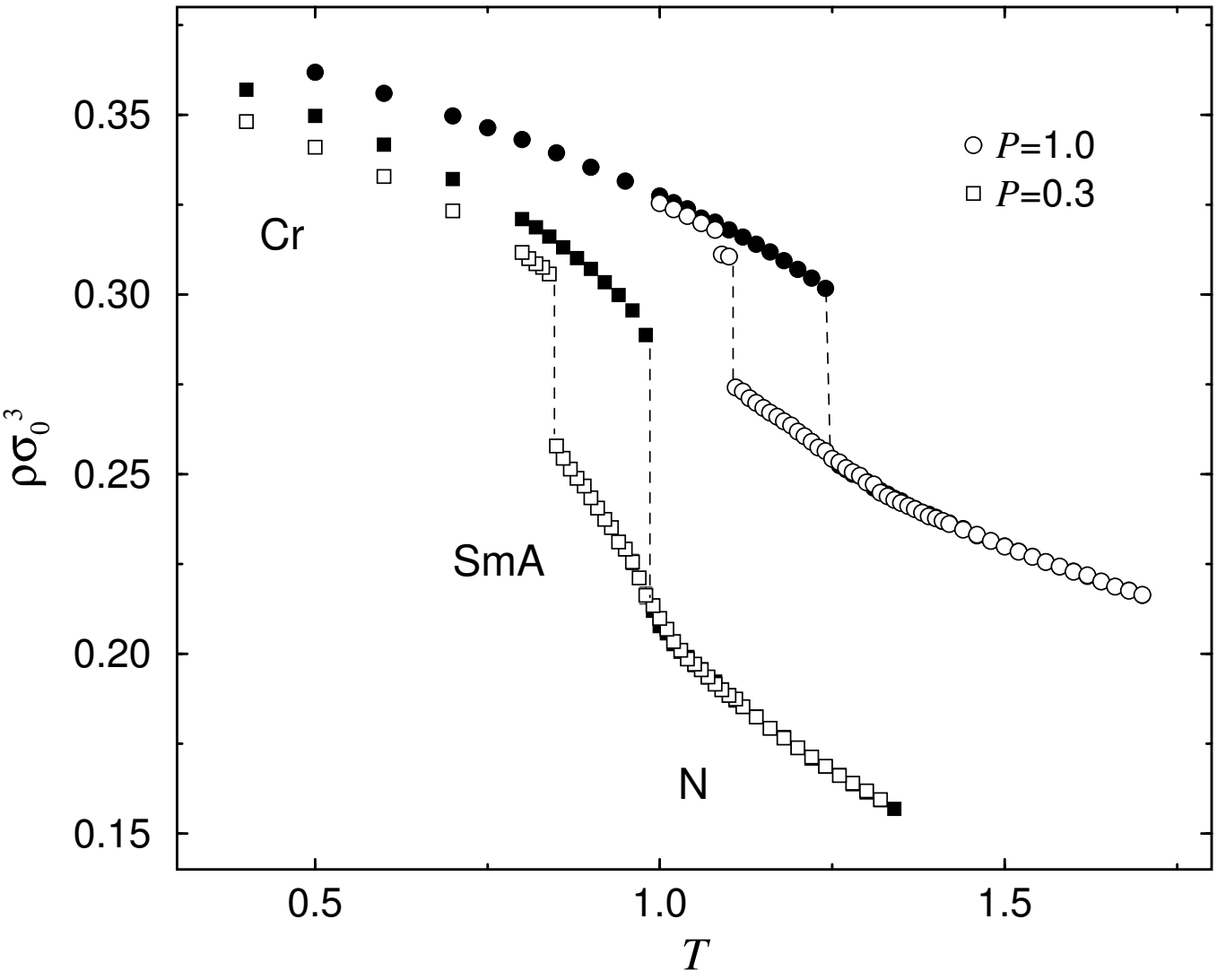

Figure 7

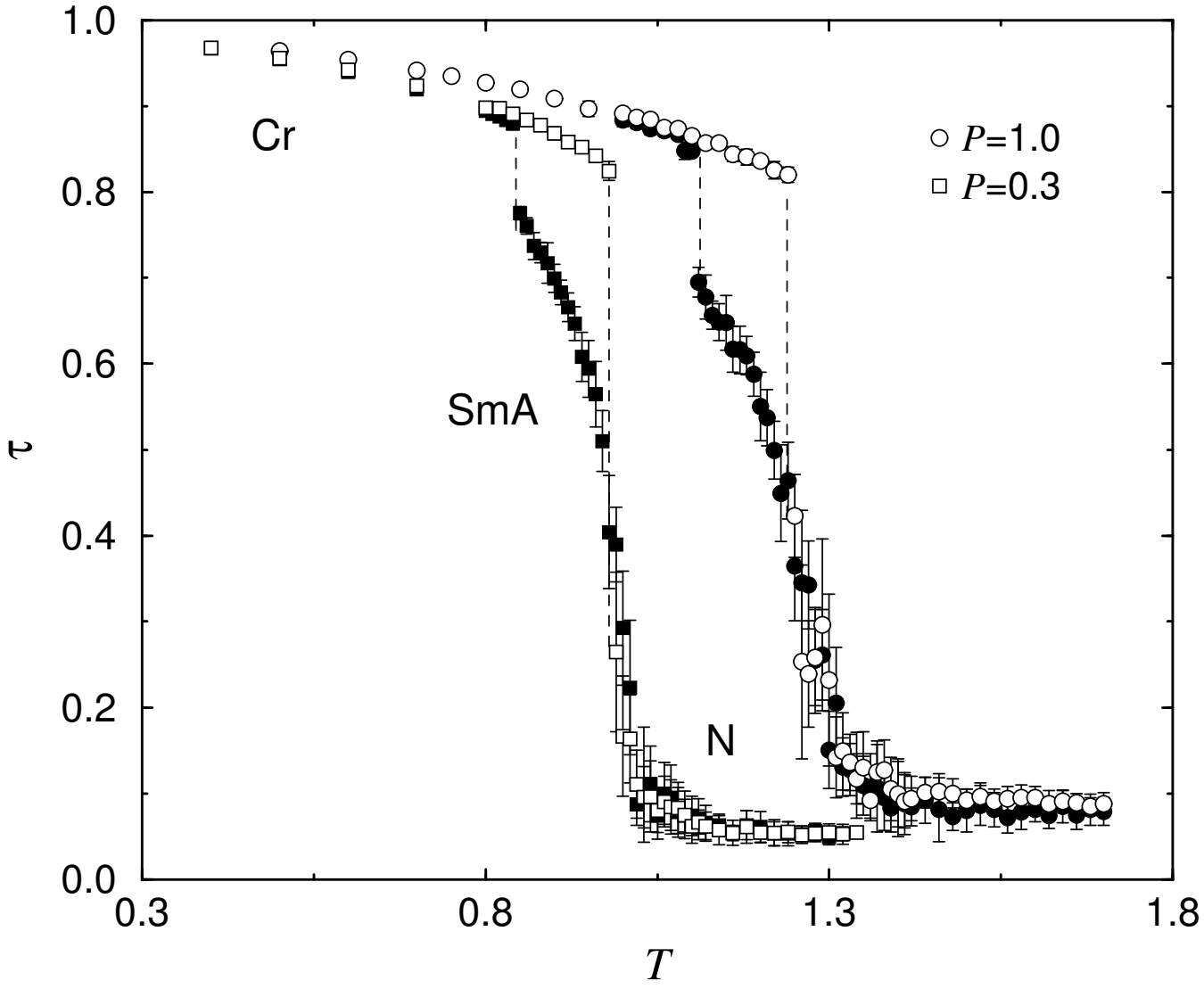

Figure 8